International Journal of Pharmaceutics 361 (2008) 78–86

Contents lists available at ScienceDirect

International Journal of Pharmaceutics

journal homepage: www.elsevier.com/locate/ijpharm

The impact of experimental hyperlipidemia on the distribution and metabolism of amiodarone in rat

Anooshirvan Shayeganpour, Hesham Korashy, Jigar P. Patel, Ayman O.S. El-Kadi, Dion R. Brocks*

Faculty of Pharmacy and Pharmaceutical Sciences, University of Alberta, Edmonton, Alberta, Canada T6G 2N8

ARTICLE INFO

Article history:
Received 16 April 2008
Received in revised form 15 May 2008
Accepted 19 May 2008
Available online 27 May 2008

Keywords:
Hyperlipidemia
Tissue distribution
Metabolite
Microsomes
Cytochrome P-450

ABSTRACT

The tissue distribution and hepatic microsomal metabolism of amiodarone were studied in a hyperlipidemic rat model. Rats were rendered hyperlipidemic by the intraperitoneal injection of poloxamer 407. Other normolipidemic animals given saline in place of poloxamer 407 were used as control animals. After single intravenous injection of amiodarone HCl (25 mg/kg) rats were anesthetized and plasma and tissue specimens were obtained. Liver microsomal protein was harvested and used to measure velocity of desethylamiodarone formation from amiodarone and cytochrome P450 (CYP) protein expression. Hyperlipidemia caused large increases in plasma concentrations of amiodarone. In tissues, however, concentrations of drug selectively increased, decreased or did not change. In heart, the site of action of the drug, as well as liver and spleen, amiodarone concentrations increased. In other tissues such as kidney, lung and brain, concentrations decreased. No changes were seen in fat or thyroid. Decreases were observed in liver metabolic efficiency, and expression of CYP3A1/2 and 2C11. No changes were seen in CYP2B1/2, 2C6, 2D1 or 1A2. This experimental hyperlipidemia caused a complex pattern of changes in tissue distribution of AM. In addition, there are decreases in the expression of some important rat CYP isoenzymes.
© 2008 Elsevier B.V. All rights reserved.

1. Introduction

Amiodarone (AM) is an effective agent in the treatment and prophylaxis of wide range of cardiac rhythm disturbances including ventricular fibrillation and pulse-less ventricular tachycardia, refractory sustained atrial fibrillation and symptomatic atrial flutter (Vassallo and Trohman, 2007). Amiodarone extensively distributes to body tissues due to its lipophilic structure, lending itself to a very high volume of distribution (Hosaka et al., 2002). In humans AM also has moderate to low bioavailability, a low hepatic extraction ratio, and a long elimination half-life, likely due to its extensive distribution to tissues (Riva et al., 1982a,b; Shayeganpour et al., 2007a). The rat shares many of the pharmacokinetic characteristics of AM with human, except that its hepatic extraction ratio is higher (Shayeganpour et al., 2007a; Shayeganpour et al., 2005). In both species AM is extensively metabolized, with the prevalent metabolite being desethylamiodarone (DEA), which is a product of mono-deethylation of AM by CYP (Fabre et al., 1993; Shayeganpour et al., 2006). Similar to AM, the chemical structure of DEA also confers it with properties of high lipophilicity and associated high volume of distribution (V_{dss}). In the rat, DEA has been shown to have a higher plasma clearance (CL) than the parent drug (Shayeganpour et al., 2007a).

Desethylamiodarone shares some of the pharmacological and toxicological properties of the parent drug. For instance, in heart DEA significantly increases the action potential duration and decreases the maximum rate of depolarization at clinically relevant concentrations (Varbiro et al., 2003). Also, DEA shows substantial effects on fast channel tissues (Talajic et al., 1989). In addition, both AM and DEA may be associated with the development of pulmonary, thyroid, ocular and liver toxicities (Basaria and Cooper, 2005; Vassallo and Trohman, 2007). In humans, DEA appears to be associated with higher myocardial concentrations than parent drug (Candinas et al., 1998), thus contributing to an increased potency of AM.

Hyperlipidemia (HL), which is a prevalent predisposing factor for cardiovascular disease, has been shown to play an important role in the pharmacokinetic properties of AM. Data from this laboratory has shown that in an experimental model of HL, the pharmacokinetic properties of AM CL and V_{dss} could be markedly reduced (Shayeganpour et al., 2005). It was also demonstrated that the unbound fraction of AM was significantly lower in the presence of HL, which was in line with the observed changes in pharmacokinetics. In both human and rat HL plasma, there was a shift of drug into the triglyceride (TG) rich lipoprotein fractions (Shayeganpour et al., 2007b). Although there is some understanding of the changes

* Corresponding author. Tel.: +1 780 492 2953; fax: +1 780 492 1217.
E-mail address: dbrocks@pharmacy.ualberta.ca (D.R. Brocks).

0378-5173/$ – see front matter © 2008 Elsevier B.V. All rights reserved.
doi:10.1016/j.ijpharm.2008.05.019

that occur in plasma in response to HL, there is no information available as to the effects of elevated plasma lipoproteins on the concentrations of AM in tissues. Because lipoproteins possess apoproteins, which are recognized by tissue lipoprotein receptors, within their structure, it is conceivable that there could be distribution of drug into tissues unexpected based on the changes in unbound fraction (Wasan et al., 2008), as has been specifically observed for cyclosporine A (Aliabadi et al., 2006). Hyperlipidemia may also potentially influence the metabolism of a drug such as AM, because of data showing that there may be a down-regulation of some CYP isoenzymes in the Zucker obese rat (Kim et al., 2004).

The intraperitoneal (i.p.) injection of poloxamer 407 (P407) to rats (1 g/kg) causes a profound but reversible rise in circulating lipoprotein levels by modification of a number of biochemical pathways (Wasan et al., 2003). Although P407 represents an extreme model of HL, it is without apparent toxicities, and is one of the few that has been shown to able to cause atherosclerosis in rodents (Palmer et al., 1997). This provides it a unique status as an animal model of HL. To better understand the potential effects of HL on the tissue uptake of both AM and its active metabolite DEA after single doses, we undertook biodistribution and metabolism assessments using this model, the results of which are described here. We also examined the influence of our animal model of HL on the expression of some CYP isoenzymes possibly contributing to the metabolism of the drug.

2. Materials and methods

2.1. Chemicals

Amiodarone HCL (AM), cholesterol (CHOL) and P407 were obtained from Sigma (St. Louis, Mo, USA). Desethylamiodarone (DEA) was obtained as a gift from Wyeth Ayerst (Research Monmouth Junction, NJ, USA). Halothane BP was purchased from MTC Pharmaceuticals (Cambridge, Ontario, Canada). Heparin sodium injection was obtained from Leo Pharma Inc. (Thornhill, Ontario, Canada). Amiodarone HCL for injection was from Sabex (Quebec, Canada). Antibodies for rat CYP1A2, CYP2B1/2, CYP2C6, CYP3A1 and actin, secondary IgG with horseradish peroxidase and low range markers were purchased from Santa Cruz Biotechnology Inc. (Santa Cruz, CA). Antibodies for rat CYP2C11, CYP2D1 and CYP3A2 were purchased from Cedarlane Laboratories Limited (Hornby, Ontario, Canada).

2.2. Animals and pre-experimental procedures

All experimental protocols involving animals were approved by the University of Alberta Health Sciences Animal Policy and Welfare Committee. A total of 80 male Sprague–Dawley rats (Charles River, CRC, Quebec, Canada) were used in the studies. Body weight was between 250 and 350 g and all of the rats were housed in temperature controlled rooms with 12 h light per d. The animals were fed a standard rodent's chow containing 4.5% fat (Lab Diet 5001, PMI nutrition LLC, Brentwood, USA). Free access to food and water was permitted prior to experimentation.

In order to assess the effect of HL on the disposition of AM, rats were allocated into two groups of normolipidemia (NL) and HL. About 36 h before the tissue distribution experiment, one group of rats was rendered HL by single intraperitoneal administration of 1 g/kg P407 (0.13 g/mL solution in cold normal saline). To ensure the proper injection of the dose, the animals were lightly anesthetized with halothane, injected with P407 and allowed to recover. The same amount of normal saline was injected intraperitoneally to NL animals under halothane.

The d after the i.p. injection, the right jugular veins of all rats were catheterized with Micro-Renathane tubing (Braintree Scientific, Braintree, MA) under halothane anesthesia. The cannulae were filled with 100 U/mL heparin in 0.9% saline. After implantation, the animals were transferred to regular holding cages and allowed free access to water and food. The next morning the rats were transferred to metabolic cages and dosing with AM was performed.

2.3. Amiodarone administration and sample collection

Amiodarone was injected i.v. through the jugular vein cannula. The doses were prepared by dilution of AM i.v. solution in normal saline to a final concentration of 12.5 mg/mL. Rats in each group received 25 mg/kg of AM. The i.v. doses were injected over 60 s via the jugular vein cannulae, immediately followed by injection of approximately 1 mL of sterile normal saline.

Animals in each group were anesthetized under halothane ($n = 4$ per time point) at approximately 0.083, 1, 2, 6, 12, 24 and 72 h postdose. At each time point, plasma, heart, liver, kidney, lung, brain, fat and spleen were harvested and kept at −30 °C until assayed for AM and DEA.

In two separate groups of NL and HL rats ($n = 4$ per group), following the administration of 25 mg/kg of drug, the thyroid glands were excised under anesthesia at 24 h postdose and kept at −30 °C freezer until assayed for AM and DEA.

2.4. Characterization of microsomal DEA formation

For in vitro studies, four male Sprague–Dawley rats in each group (NL and HL) were sacrificed under anesthesia and their livers were excised. Microsomal protein from homogenized tissue was prepared by differential ultracentrifugation. The final pellets were collected in cold sucrose and stored at −80 °C. Microsomes from each rat were prepared separately and were used to characterize the kinetics of the in vitro formation of DEA from AM and the effect of HL on the DEA formation as previously described (Shayeganpour et al., 2006). The Lowry method was used to measure the total protein concentration in each microsomal preparation (Lowry et al., 1951). Total CYP was measured (Omura and Sato, 1964) in each rat liver microsomes and the results of NL and HL compared.

Each 0.5-mL incubate contained 1 mg/mL protein from each of the microsomal preparations from the four individual rats, 1 mM NADPH, and 5 mM magnesium chloride hexahydrate dissolved in 0.5 M potassium phosphate buffer (pH 7.4). Amiodarone was dissolved in methanol and added to the liver microsomal suspension (8 μL/mL). The oxidative reactions were started with the addition of NADPH after a 5-min preequilibration period. Each incubation was performed in duplicate in a 37 °C water bath shaker for 30 min. Incubation conditions were optimized so that the rate of metabolism was linear with respect to incubation time and microsomal protein concentration. The amount of AM spiked into each incubation mixture yielded a range of concentrations from 0.1 to 230 μM (equivalent to 0.065–148 μg/mL).

To determine the direct effect of P407 on hepatic metabolism of AM to DEA, 5 mg/mL of P407 dissolved in normal saline was added to a series of tubes containing 1 mg/mL of NL hepatic microsomes. Incubation was carried out with 50 μM of AM at 37 °C for 30 min at the presence of NADPH. The generated DEA was determined and the results compared with control incubations without P407.

2.5. Western blot analysis

Western blot analysis was performed using a previously described method with minor modification to quantify the effect of HL on some important CYP isoenzymes including

CYP1A2, CYP2B1/2, CYP2C6, CYP2C11, CYP2D1, CYP3A1 and CYP3A2 (Korashy and El-Kadi, 2004). Briefly, 100 μg of each individual microsomal protein was denatured by diluting with loading buffer and boiling for 5 min at 100 °C. Then each sample was loaded onto a 10% SDS-polyacrylamide gel and subjected to electrophoresis at 120 V for 2 h. The separated proteins were transferred to Trans-Blot nitrocellulose membrane (0.45 μm) in a buffer containing 25 mM Tri–HCl, 192 mM glycine, and 20% (v/v) methanol. Protein blots were blocked overnight at 4 °C in a solution containing 5% skim milk powder, 2% bovine serum albumin and 0.5% Tween-20 in Tris-buffered saline buffer. Thereafter, the blocking solution was removed and the blots were rinsed three times in a wash buffer (0.1% Tween-20 in TBS). Membranes were incubated with primary antibodies (1/500 or 1/1000 dilution) to either rat CYP1A2, CYP2B1/2, CYP2C6, CYP2C11, CYP2D1, CYP3A1 and CYP3A2 for 2 h at 4 °C in TBS containing 0.01% sodium azide and 0.05% Tween-20. The primary antibody solution was removed and blots were rinsed three times with a wash buffer, followed by incubation with horseradish peroxidase conjugated with rabbit or mouse anti-goat IgG secondary antibody (1/5000 dilution) for 1 h at room temperature and washed. Immunoactive proteins were detected using the enhanced chemiluminescence method (Amersham, Arlington Heights, IL) and the intensity of different CYP protein bands were quantified, relative to the signals obtained for actin, using Java-based image-processing software, ImageJ (W. Rasband [2005] National Institutes of Health, Bethesda, MD, http://rsb.info.nih.gov/ij).

2.6. Assay of plasma lipids

Total CHOL and TG concentrations were determined using enzymatic CHOL and TG assay kits. Two milliliters of CHOL or TG reagents was added to 10 μL of rat NL or HL plasma samples. Tubes were incubated at 37 °C for 5 or 10 min and scanned at 505 or 515 nm, respectively using an ultraviolet spectrophotometer.

2.7. Assay of AM and DEA

A validated LC–MS method was used to measure the plasma and tissue concentrations of both AM and DEA (Shayeganpour et al., 2007c). The assay had a validated lower limit of quantification of 2.5 ng/mL for both AM and DEA in 100 μL of rat plasma and 5 ng/g of both AM and DEA in each of the selected rat tissues. Separate calibration curves were made for each tissue for quantitation of AM and DEA in the same tissue type. The method was modified to assay both AM and DEA in microsomal protein. Denatured microsomal media and blank tissues were used and spiked for standard curve preparation. Briefly to each tube containing 500 μL of microsomal incubation mixture and 1.5 mL of acetonitrile, 30 μL of internal standard (2.5 μg/mL ethopropazine HCl) was added. The tubes were vortex mixed for 30 s and centrifuged for 2 min at 2500 × *g*. The supernatant was transferred to new glass tubes, 7 mL of hexane was added, and the tubes were vortex mixed for 45 s and centrifuged for 3 min. The organic layer was transferred to new tubes and evaporated to dryness in vacuo. The dried residue was reconstituted by adding 1 mL of pure methanol and aliquots of 5–10 μL were injected into the LC/MS apparatus. For standard curves, drug-free microsomal preparations of liver or intestine without NADPH were used and spiked with appropriate amounts of AM and DEA. The CV% of the assay was less than 20%.

2.8. Data analysis

The mean area under the tissue or plasma versus time curves (AUC) from time of dosing to last measured time point was determined by the combined log-linear trapezoidal rule. The tissue to plasma AM or DEA concentration ratios (K_p) were determined for the AUC, and for the concentrations during the terminal elimination phase, which appeared from 24 h onwards after the AM was administered. It is during this postdistributive phase that constant tissue to plasma concentration ratios are expected to be reached. Previously it was estimated that mean unbound fractions of AM in plasma from NL and P407-treated rats were 0.147 and 0.00345%, respectively (Shayeganpour et al., 2005). These unbound fractions were multiplied by the plasma AUC and used to permit an estimate of the K_{pu}, which is the tissue to unbound plasma concentration ratio.

Rates of DEA formation in liver microsomes were obtained by plotting the formed DEA versus AM concentrations. Single enzyme models for metabolism of AM to DEA were fitted to the formation rate versus time data using nonlinear curve-fitting routines using an in-house written program based on Microsoft Excel (Microsoft, Redmond, WA) and the Solver routine. The Michaelis–Menten model for a single enzyme was used as follows:

$$\text{Rate of DEA formation} = \frac{V_{max} \times [AM]^n}{K_m^n + [AM]^n}$$

where V_{max} is the maximal rate of formation (capacity), K_m is the affinity constant, [AM] is AM concentration, and n is the shape factor required to fit sigmoidal shapes. When $n = 1$, the model reduced to the simple Michaelis–Menten equation. In the presence of sigmoidal relationships, the maximum clearance (CL_{max}), which was obtained graphically from the highest value of rate/[AM] noted in the clearance (rate/[AM] vs. [AM]) plot (Houston and Kenworthy, 2000; Vuppugalla and Mehvar, 2005), and used as the most appropriate measure of intrinsic clearance (CL_{int}).

2.9. Statistical analysis

Compiled data were expressed as mean ± S.D. unless otherwise indicated. In the tissue distribution study, AUC for AM and DEA were determined for each specimen. The S.D. of partial AUC was estimated to assess significance of differences (Bailer, 1988). In this test, α was 0.05, the critical value of Z (Z_{crit}) for the 2-sided test after Bonferroni adjustment was 2.24, and the observed value for Z (Z_{obs}) was calculated.

For microsomal studies, Western blot analysis, and postdistributive K_p and K_{pu}, the Student's paired or unpaired t tests were used as appropriate to assess the significance of differences between NL and HL groups. Microsoft Excel was used in statistical analysis of data. The goodness of fit was measured using Akaike Information Criterion and least sum of squares. The level of significance was set at $p = 0.05$ for all comparisons.

3. Results

3.1. Biodistribution experiments

In the plasma of NL rats, the total TG and CHOL concentrations were 0.549 ± 0.219 and 1.03 ± 0.356 mM, respectively. In contrast, in the plasma of HL rats, the total TG (46.7 ± 18.6 mM) and CHOL (29.3 ± 6.97 mM) concentrations were substantially and significantly higher.

Both AM and DEA were detected in all of the tissues. After single-dose i.v. administration of AM to all rats, the plasma concentrations initially rapidly declined. By 12 h after dosing the terminal phase appeared to be log-linear, indicating that postdistributive conditions had been reached (Fig. 1). In all of the NL tissues except for fat, there was no evidence of delayed tissue absorp-

tion as the first concentration at 5 min postdose was the highest. In contrast, delayed tissue concentrations of AM were noted in the lung, kidney, spleen, and fat of HL animals. For most corresponding sample times the plasma concentrations were higher in HL than NL rats, and the plasma concentrations in the terminal phase declined more rapidly (Fig. 1). For specific tissue concentrations versus time profiles, shapes generally were similar for the HL and NL groups, although in some tissues concentrations were higher in HL animals, and in others the reverse was the case.

For DEA similar to AM, the DEA plasma concentrations in the terminal phase declined more rapidly in the HL animals. However,

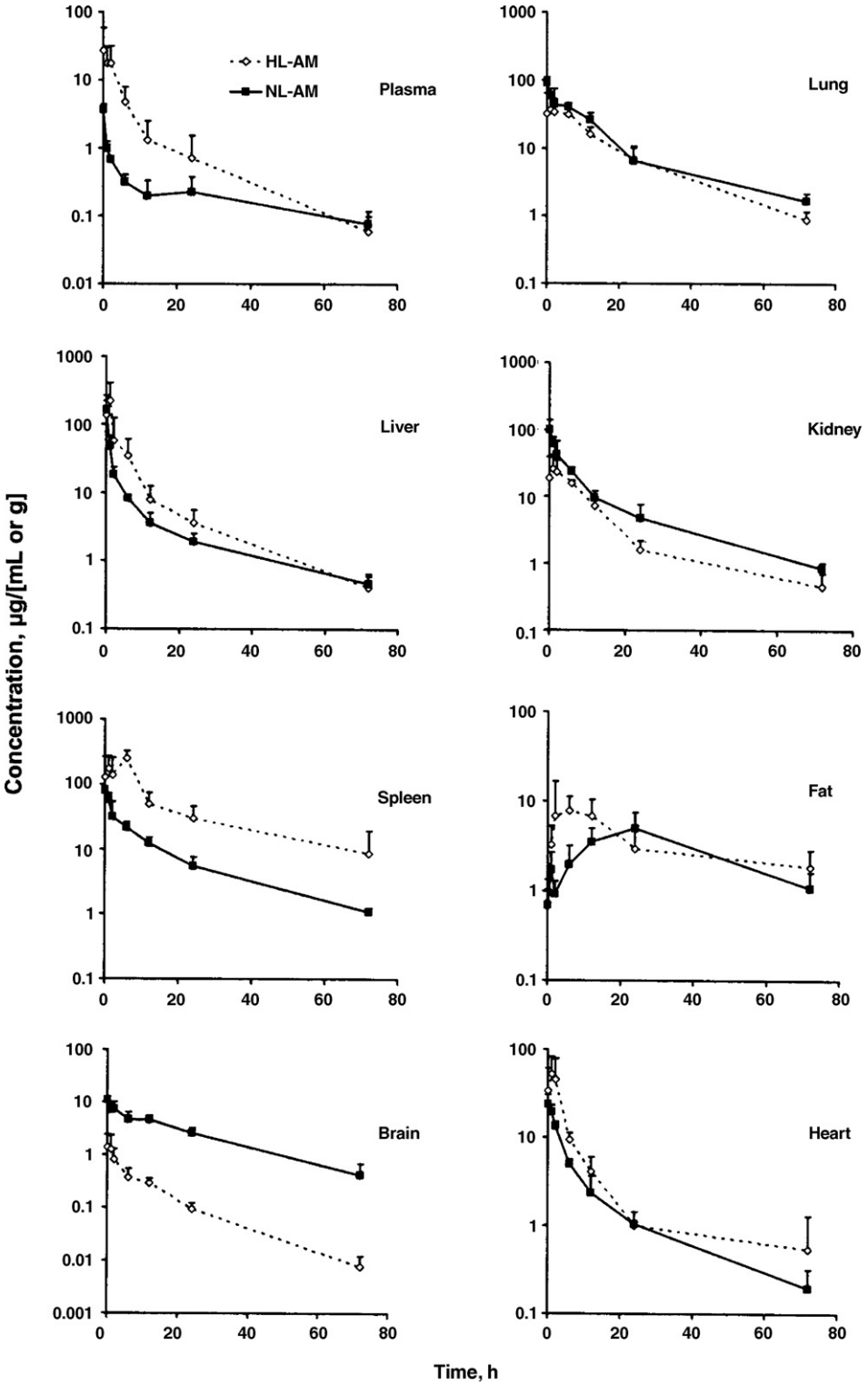

Fig. 1. Amiodarone concentration vs. time profiles in tissues following single intravenous administration of 25 mg/kg in normolipidemic (NL) and hyperlipidemic (HL) rats. *Significant differences between NL and HL rats.

at all time points plasma concentrations were higher for the HL rats (Fig. 2). In NL animals there was evidence of delayed appearance of DEA in kidney, spleen, fat, brain and heart. In HL delayed appearance of DEA was evident in all of the tissues, including the plasma. The delay was in general much more noticeable in the HL rats.

Compared to NL (Table 1), HL was associated with significantly higher AM and DEA plasma AUC (8- and 23-fold, respectively). The AUC of AM was also significantly increased in heart (two-fold), liver (2.5-fold) and spleen (5.6-fold). In contrast, in HL brain, kidney and lung the measured AM AUC were significantly decreased by 94, 50 and 47%, respectively (Fig. 1, Table 1). For DEA, there were no

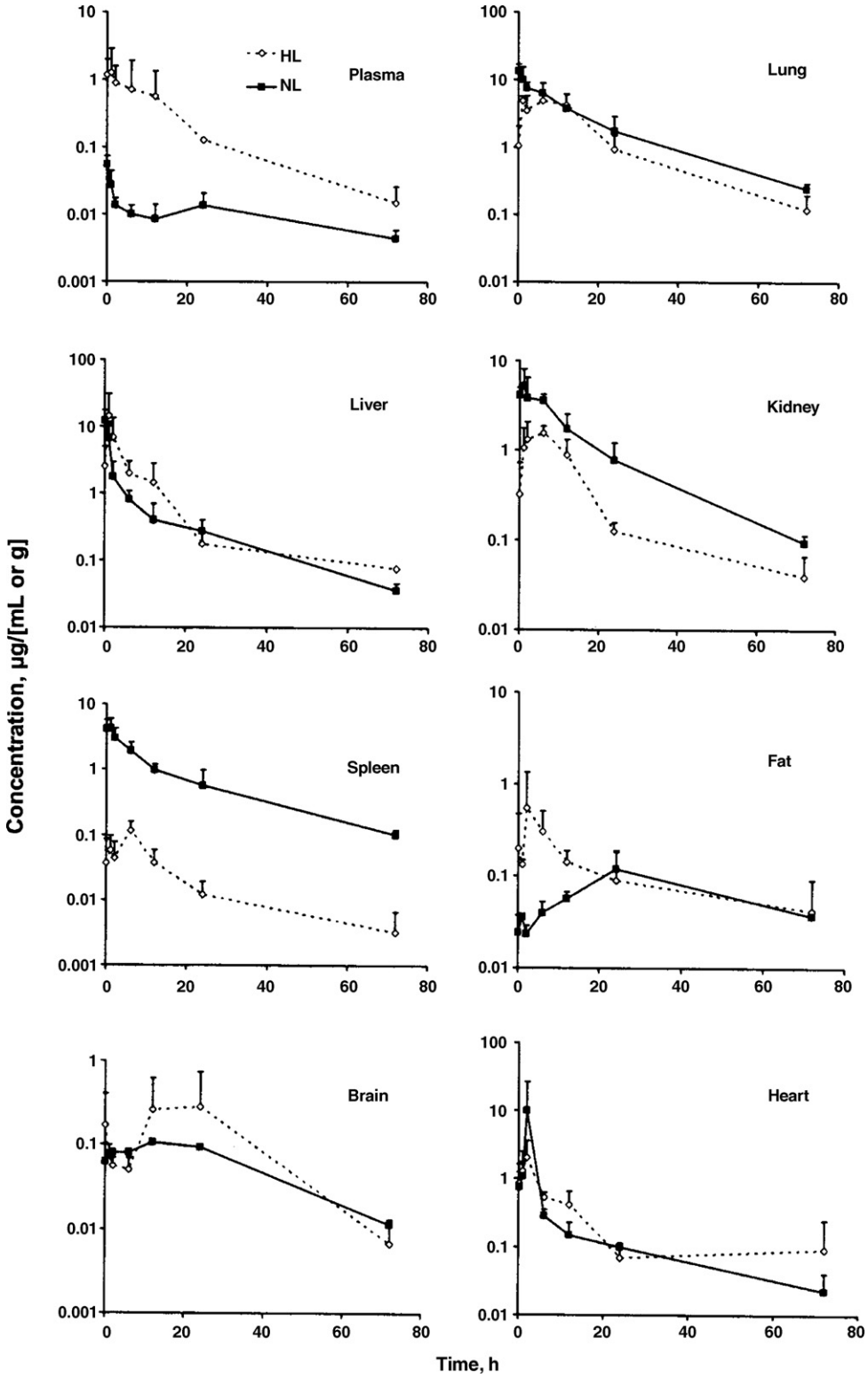

Fig. 2. Desethylamiodarone concentration vs. time profiles in tissues following single intravenous administration of 25 mg/kg amiodarone in normolipidemic (NL) and hyperlipidemic (HL) rats. *Significant differences between NL and HL rats.

Table 1
Tissue uptake of AM and DEA in NL and HL rats given 25 mg/kg i.v. bolus doses of AM HCl

Tissue	AUC_{0-72}								K_p	
	AM			DEA			DEA:AM		NL	HL
	NL	HL	HL:NL ratio	NL	HL	HL:NL Ratio	NL	HL		
Plasma	16.7 ± 2.38	134 ± 25.8*	8.0	0.728 ± 0.112	17.0 ± 5.37*	23	0.0436	0.126	–	–
Brain	182 ± 12.5	11.4 ± 1.17*	0.063	4.72 ± 0.636	11.5 ± 8.01	2.4	0.0259	1.01	10.9	0.0851
Heart	146 ± 17.4	279 ± 49.2*	1.9	32.6 ± 23.6	17.3 ± 3.20	0.53	0.223	0.0620	8.74	2.08
Kidney	577 ± 55.7	289 ± 25.0*	0.50	75.3 ± 8.36	24.8 ± 2.44*	0.33	0.131	0.0858	34.6	2.16
Liver	313 ± 22.3	786 ± 146*	2.5	33.0 ± 4.05	62.3 ± 14.1	1.9	0.105	0.0793	18.7	5.87
Lung	924 ± 73.6	478 ± 61.8*	0.52	159 ± 20.8	82.5 ± 12.8*	0.52	0.172	0.173	55.3	3.57
Fat	222 ± 41.5	253 ± 45.1	1.1	5.28 ± 1.06	8.09 ± 2.21	1.5	0.0238	0.0320	13.3	1.89
Spleen	607 ± 38.2	3373 ± 382*	5.56	51.9 ± 6.69	1.54 ± 0.191*	0.030	0.0855	0.0060	36.3	25.2

The mean ± S.D. of the AUC_{0-72} (μg h/[mL or g]) of AM and DEA are shown. Asterisks represent significant differences in AUC from NL.

significant increases in AUC noted in any HL tissue. However, in HL kidney, lung and spleen there were significant decreases of 67, 47 and 97% fold, respectively in the AUC of DEA (Fig. 2, Table 1). In thyroid, no significant differences were observed between the concentrations of AM and DEA in NL and HL rats 24 h postdose (Fig. 3).

The calculated K_p for the AM AUC in HL animals were consistently lower those in NL animals (Table 1). For DEA the postdistributive K_p in HL were numerically lower than NL for all tissues except heart. The estimated K_{pu} of AM AUC in NL rats yielded mean values of 7413, 5947, 23,504, 12,750, 37,639, 9043 and 24,726 in brain, heart, kidney, liver, lung, fat and spleen, respectively. In contrast, in HL tissues the corresponding K_{pu} were 2466, 60,350, 62,513, 170,020, 103,396, 54,726 and 729,613, respectively. The mean K_{pu} in HL was therefore higher than NL in all tissues except for brain.

The calculated AUC ratios of DEA:AM in several of the HL tissues (heart, kidney, liver and spleen) were lower than in NL specimens (Table 1). In lung the mean DEA:AM AUC ratios in both NL and HL animals were equal. In brain however, the AUC ratio of DEA:AM in HL was 39-fold higher than that of NL rats. Plasma and fat had somewhat higher mean DEA:AM AUC ratios in the HL animals as well (Table 1).

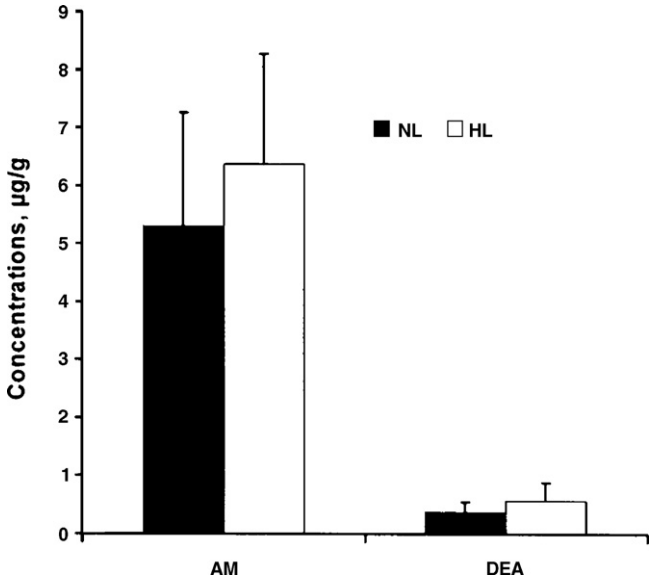

Fig. 3. The concentrations of amiodarone (AM) and desethylamiodarone (DEA) in thyroid glands 24 h postdose in NL and HL animals given 25 mg/kg AM. No differences were seen between NL and HL animals.

3.2. Hepatic microsomal metabolism of AM to DEA

In the preliminary evaluation of microsomal metabolism it was noted that at a single concentration the formation rate of DEA from AM was less in microsomal protein of HL rats. This prompted a more complete metabolic characterization of the drug in rat hepatic microsomes using a wider range of concentrations than was previously used (Shayeganpour et al., 2006). The kinetic profile of DEA formation versus concentration conformed best to the sigmoidal Michaelis–Menten model with one enzyme (Fig. 4A). Eadie–Hofstee plots of both NL and HL data displayed convexity suggesting sigmoidal kinetics (Fig. 4B). The fit of the sigmoidal model to the data was improved over the simple non-sigmoidal model, and the two enzyme Hill equation. The CL_{max} was therefore estimated by plotting the data in clearance plots as depicted in Fig. 4C.

The estimated K_m, V_{max}, and clearance maximum (CL_{max}) were determined in each of the liver microsomal specimens (Table 2). There were higher apparent rates of DEA formation in NL than in HL (Fig. 4A). There were no significant differences discernable between the K_m and the V_{max} of NL and HL rat hepatic microsomes (Table 2). There was a higher degree of variability in the estimated V_{max} and in particular K_m in HL compared to NL. In contrast, for CL_{max} the variability was the same for both NL and HL, and the difference was significant between groups, with NL being greater than HL (1.46-fold).

When P407 was added directly to the microsomal incubates, there was no significant impact on the formation of DEA from AM. The formation rates were 91.3 ± 9.82 and 89.4 ± 10.4 pmol/(min mg protein) in the absence and presence of P407, respectively.

3.3. CYP expression

The total CYP content was significantly lower in microsomal protein from HL (0.407 ± 0.0883) than NL (0.788 ± 0.183 nmol/mg protein) livers (Fig. 5), which prompted an investigation of CYP

Table 2
Enzyme kinetic parameters for desethylamiodarone formation by normolipidemic (NL) and hyperlipidemic (HL) liver microsomes from four individual rats (mean ± S.D., range in parentheses)

	NL	HL
K_m (μM)	102 ± 16.3 (79.7–118)	143 ± 85.3 (77.0–266)
V_{max} (pmol/(min mg protein))	387 ± 69.6 (327–473)	306 ± 86.1 (230–416)
CL_{max} (μL/(min mg protein))	2.12 ± 0.349 (1.66–2.59)	1.48 ± 0.251* (1.14–1.71)

*Significant differences from NL (Student's unpaired t-test, $p < 0.05$).

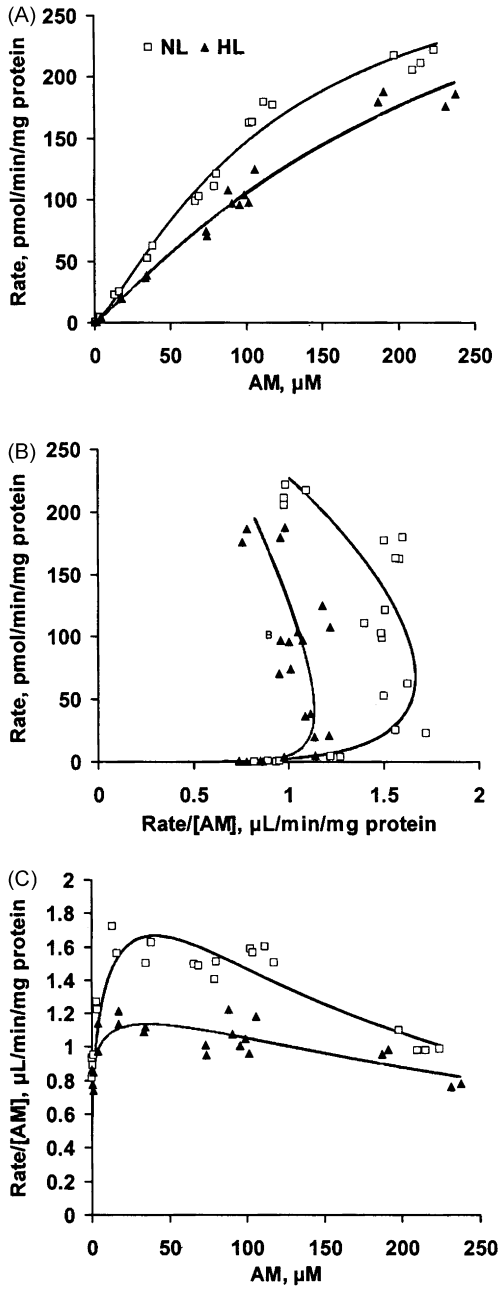

Fig. 4. Plots of (A) velocity of formation vs. amiodarone (AM) concentration, (B) Eadie–Hofstee and (C) clearance plots in formation of desethylamiodarone from AM by NL and HL liver microsomes from a representative Sprague–Dawley rat.

protein expression in the microsomal preparations. Western blot analysis for CYP2C11, CYP3A1 and CYP3A2 showed significant decreases of 39.6, 51.9 and 38.4%, respectively, in the hepatic microsomes of HL rats compared to NL rats. On the other hand the expression of CYP 1A2, 2B1/2, 2C6 and 2D1 did not change (Fig. 5).

4. Discussion

This is the first data describing the influence of HL on the tissue uptake of AM and DEA. As expected (Shayeganpour et al., 2005), the plasma total AM AUC in HL were much higher than that in NL. Previously (Shayeganpour et al., 2005) an assay was used that limited the ability of DEA to be measured in plasma. Here with a more sensitive assay, full plasma AUC of DEA were determinable in both NL and HL rats (Fig. 2). In the tissues it was observed that HL caused AM concentrations to significantly increase in some tissues, including heart, the site of action of the drug (Table 1). Potentially this could imply that HL causes an increased effect of the drug on its cardiac effects. In this respect, it is of note that a nice modeling of the AM concentration versus inotropism relationship has been demonstrated with amiodarone (Sermsappasuk et al., 2006). In contrast, lower concentrations were observed in lung, a site of toxicity of AM (Fig. 1, Table 1). Although only one timed sample was obtained, for another organ associated with side effects, thyroid, there was no change in AM uptake in HL (Fig. 3).

Based on the estimates of unbound fraction (Shayeganpour et al., 2005), assuming linear binding over the course of the plasma concentration versus time profile, it was estimated that the mean unbound AUC of AM in NL and HL rats were approximately 25 and 4.3 ng h/mL, respectively, thus representing an approximately 5.75-fold higher unbound AUC in NL versus HL rats. This use of our unbound fraction calculations established earlier (Shayeganpour et al., 2005) is reasonable considering that in rats given three escalating oral dose regimens (25, 50 and 100 mg/(kg d) × 13 d) there were increases noted in the mean serum concentrations across the range of doses (Plomp et al., 1985), suggesting that nonlinear protein binding does not occur. Therefore, in HL, given its lower unbound concentrations, AM might be expected to be associated with across the board decreases in the distribution to the peripheral tissues, given its moderate hepatic extraction ratio in rat. Indeed, the volume of distribution of AM was reduced 23-fold in the HL state in line with the change in unbound fraction previously described (Shayeganpour et al., 2005). Consistent with this change, in brain, kidney, and lung significant decreases were seen in total AM uptake. These expected observations, however, were not uniformly seen in all tissues. Indeed in some HL tissues, including the liver, spleen, and notably the target organ for effect of the drug, the heart, AUC were significantly higher.

In general, the observed relative tissue:plasma total drug AUC ratios (Table 1) matched well with the values reported earlier in NL Sprague–Dawley rats given radiolabeled AM 50 mg/kg i.v. (Wyss et al., 1990). In the HL rats, lower K_p were seen for each of the tissues studied (Table 1), although the K_p between tissues differed widely. Such a reduction in K_p was previously observed for cyclosporine A in the same P407 rat model of HL (Aliabadi et al., 2006). Given that uptake of drug into tissues is normally dependent to some degree on the plasma unbound fraction, the K_{pu} were calculated and compared. If unbound fraction alone was responsible for the uptake of the drug by tissues, there should be little difference between HL and NL in this parameter. However, in all cases except for brain the K_{pu} was higher for HL than corresponding NL tissues. Although statistical comparison of the K_{pu} AUC was not possible, by examining those concentrations during the postdistributive phase (24 h or longer) from each of the tissues, it was apparent that for all tissues except for brain the K_{pu} of HL rats were significantly higher than NL. This suggests that unbound fraction by itself was not the only controlling factor for tissue uptake of the drug in HL. Although the study design does not allow for a definitive answer to this anomaly, a feasible explanation for the increases in K_{pu} is apoprotein-mediated recognition of lipoprotein remnants containing AM (Diard et al., 1994; Shayeganpour et al., 2007b; Wasan et al., 2008).

The highest association of AM in HL rat plasma is in the TG-rich lipoprotein fraction, which is rich in chylomicron (CM) and very low-density lipoproteins (VLDL) (Shayeganpour et al., 2007b). The association of AM in low-density lipoprotein (LDL) was the second highest after TRL fraction in HL rat plasma (Shayeganpour et al., 2007b). This might help explain the high AM AUC in some tissues such as liver, heart and spleen of HL rats. It is known that VLDL receptor mRNA is highly expressed in specific tissues. The

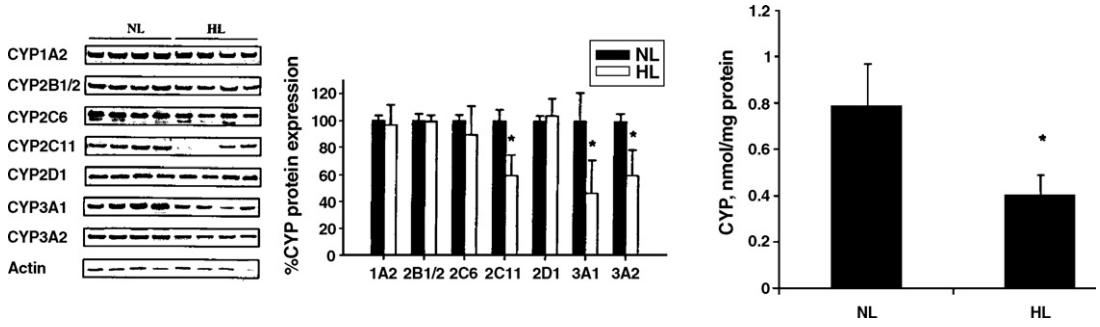

Fig. 5. The effect of hyperlipidemia (HL) on expression of different CYP enzymes in Sprague–Dawley rat liver microsomes shown by Western blot (left and centre panels), and total CYP (right panel). *Significant differences between NL and HL.

VLDL receptor mRNA levels in heart are highest, followed by muscle, kidney, adipose tissue, brain and macrophages of adult mouse (Tiebel et al., 1999). In contrast, the mRNA level of VLDL receptors was barely detectable in liver of adult mouse. In neonatal rat liver, however, the expression of VLDL receptor mRNA was about 3-fold higher (Tiebel et al., 1999). In contrast to VLDL, LDL receptors were found abundantly expressed in liver (Chung and Wasan, 2004). Given the increased association of AM to VLDL and LDL in HL (Shayeganpour et al., 2007b), the similarity in the tissue localization of LDL and VLDL receptors is in line with the observation. The high capacity of bone marrow and spleen macrophages to clear CM particles from the rat blood circulation has been demonstrated (Hussain et al., 1989). Such a mechanism might have been responsible for increased uptake of AM by spleen in HL (Fig. 1, Table 1).

The effect of HL on the biodistribution of AM in this animal model yielded some interesting differences from another LP-bound drug, cyclosporine A. For AM here it was found that AUC were increased in heart and spleen, but decreased in kidney. These findings were opposite to those seen for cyclosporine A (Aliabadi et al., 2006). Only in liver was HL associated with similar relative outcomes (increased AUC compared to NL). In the obese Zucker rat, kidney levels of amphotericin B were substantially higher than in control lean rats (Vadiei et al., 1990). HL appears to affect pharmacokinetics of lipoprotein bound drugs in a drug-specific manner. It is not possible to definitively explain these differences although drug-specific alterations in binding to specific lipoprotein classes in HL might be a cause of the differences. For example, although it is known what the plasma lipoprotein disposition of AM is in P407 HL plasma (Shayeganpour et al., 2007b), this has not been evaluated for cyclosporine A. It should be recognized that AM possesses a very long terminal phase half-life and this study only followed the distribution of the drug after a single dose (Weiss, 1999). It remains to be seen whether the distributional findings seen here also holds with chronic dosing.

Because when P407 was incubated with microsomes no change occurred in the formation of DEA from AM, the diminished metabolism of AM by microsomes does not seem attributable to a competitive interaction due to P407 itself, but rather due to the resultant HL it causes in vivo. Other models of HL caused similar observations with respect to CYP activity and/or expression (Fig. 5). For example, recently it was reported the Zucker obese rat displayed a significant decrease in the expression of a number of drug metabolizing enzymes and transport proteins (Kim et al., 2004). In the P407 model of HL the findings here (Fig. 5) suggested either suppressed expression, or increased rate of enzyme turnovers of CYP2C11, CYP3A1 and CYP3A2. Similar to the current findings, others have reported down-regulation of hepatic expression of CYP3A after high fat diet (Yoshinari et al., 2006). This down-regulation was attributed to lower expression of nuclear hormone transcription factors such as constitutive androstane receptor (CAR) and retinoid X receptor (RXR) (Yoshinari et al., 2006). In addition, it has been reported that the expression of CAR in obese Zucker rats is significantly lower than control lean rats (Xiong et al., 2002). Since CYP2C11 and CYP3A1/2 are regulated by the transcription factors, CAR and PXR (Pascussi et al., 2003), we postulate that the selective down-regulation of CYP2C11 and CYP3A1/2 in the current study is due to the decrease in the expression of both transcription factors.

The clearance of (bound + unbound) AM was diminished in P407 treated rats from 1380 in NL rats to 120 mL/(h kg), a decrease of over 90% (Shayeganpour et al., 2005). Given the unbound fractions of the drug, estimates of unbound clearance of 937 and 3450 L/(h kg) can be calculated in NL and HL, respectively. In effect an apparent paradoxical increase in unbound drug clearance was realized in HL (Table 1). Each of CYP1A, CYP3A1, CYP3A2 are involved in the metabolism of AM to DEA by rat hepatic microsomes (Elsherbiny et al., 2008; Shayeganpour et al., 2006). Although there was some decrease in the effective intrinsic CL (CL_{max}) of AM to DEA (Table 2), there was a 2.5-fold higher uptake of AM to the liver (Table 1) which exceeded the reduction observed in the microsomal CL_{max} (30%). Together these findings help to explain each of (i) the significant increase in DEA concentrations and (ii) mean DEA/AM ratio in HL plasma, (iii) the high concentrations of DEA present in HL liver and (iv) the paradoxical increase in apparent AM unbound clearance.

Despite the resemblance in the trend of lipoprotein association for AM and DEA in HL rats (Shayeganpour et al., 2007b), there were some notable discrepancies between the drug and metabolite in relative uptake by different tissues of HL rats. In plasma, similar to AM, the DEA AUC was significantly and substantially higher in the HL rats. However, there were significant reductions in DEA uptake by HL spleen, lung and kidney (Table 1). This trend was opposite of parent drug for spleen and lung, where increases were observed in HL. Except for the anticipated lower unbound fraction in HL, other possible explanations for the decreases of DEA in these tissues cannot presently be provided. For brain it was of interest that in HL the DEA:AM ratio was much higher than NL. As speculation, it can be offered that as in the gut (Kimoto et al., 2007), DEA is also a substrate for brain efflux transport. This in turn might be inhibited by the elevated plasma lipid levels in HL, as it is in gut in the presence of lipids (Custodio et al., 2008).

In conclusion, the reduction in plasma unbound fraction of AM in HL could not by itself explain the precise changes in tissue distribution. Indeed, the influence of HL on AM tissue distribution was not uniform, but rather tissue-specific, and AM metabolism and some hepatic CYP expression were decreased. As is the case for any animal model, caution is necessary in extrapolating these findings to humans. This is specifically underlined here by the degree of elevation in lipoproteins in the P407 rodent model, which is much higher than would be encountered in a human HL population. Nevertheless, assuming that this model qualitatively reflects similar changes in HL patients, these finding have potential therapeutic implica-

tions. An increased delivery of AM to the heart has the potential to confer a given dose of the drug with greater potency. The increased hepatic concentrations of AM were in line with the observation that the unbound fraction decreased more than the CL of the drug (Shayeganpour et al., 2005). The decrease in AM unbound fraction and intrinsic level of hepatic CYP activity therefore might be compensated for by an increased delivery of the lipoprotein-bound drug to the liver, where metabolism could proceed at a higher overall rate.

Acknowledgement

Funding by CIHR grant MOP 67169.

References

Aliabadi, H.M., Spencer, T.J., Mahdipoor, P., Lavasanifar, A., Brocks, D.R., 2006. Insights into the effects of hyperlipoproteinemia on cyclosporine A biodistribution and relationship to renal function. AAPS J. 8, E672–E681.

Bailer, A.J., 1988. Testing for the equality of area under the curves when using destructive measurement techniques. J. Pharmacokinet. Biopharm. 16, 303–309.

Basaria, S., Cooper, D.S., 2005. Amiodarone and the thyroid. Am. J. Med. 118, 706–714.

Candinas, R., Frielingsdorf, J., Ha, H.R., Carrel, T., Turina, M., Follath, F., 1998. Myocardial amiodarone concentrations after short- and long-term treatment in patients with end-stage heart failure. Eur. J. Clin. Pharmacol. 53, 331–336.

Chung, N.S., Wasan, K.M., 2004. Potential role of the low-density lipoprotein receptor family as mediators of cellular drug uptake. Adv. Drug Deliv. Rev. 56, 1315–1334.

Custodio, J.M., Wu, C.Y., Benet, L.Z., 2008. Predicting drug disposition, absorption/elimination/transporter interplay and the role of food on drug absorption. Adv. Drug Deliv. Rev. 60, 717–733.

Diard, P., Malewiak, M.I., Lagrange, D., Griglio, S., 1994. Hepatic lipase may act as a ligand in the uptake of artificial chylomicron remnant-like particles by isolated rat hepatocytes. Biochem. J. 299 (Pt 3), 889–894.

Elsherbiny, M.E., El-Kadi, A.O.S., Brocks, D.R., 2008. The metabolism of amiodarone by various CYP isoenzymes of human and rat, and the inhibitory influence of ketoconazole. J. Pharm. Pharm. Sci. 11, 147–159.

Fabre, G., Julian, B., Saint-Aubert, B., Joyeux, H., Berger, Y., 1993. Evidence for CYP3A-mediated *N*-deethylation of amiodarone in human liver microsomal fractions. Drug Metab. Dispos. 21, 978–985.

Hosaka, F., Shiga, T., Sakomura, Y., Wakaumi, M., Matsuda, N., Kasanuki, H., 2002. Amiodarone distribution in human tissues after long-term therapy: a case of arrhythmogenic right ventricular cardiomyopathy. Heart Vessels 16, 154–156.

Houston, J.B., Kenworthy, K.E., 2000. In vitro–in vivo scaling of CYP kinetic data not consistent with the classical Michaelis–Menten model. Drug Metab. Dispos. 28, 246–254.

Hussain, M.M., Mahley, R.W., Boyles, J.K., Lindquist, P.A., Brecht, W.J., Innerarity, T.L., 1989. Chylomicron metabolism. Chylomicron uptake by bone marrow in different animal species. J. Biol. Chem. 264, 17931–17938.

Kim, M.S., Wang, S., Shen, Z., Kochansky, C.J., Strauss, J.R., Franklin, R.B., Vincent, S.H., 2004. Differences in the pharmacokinetics of peroxisome proliferator-activated receptor agonists in genetically obese Zucker and Sprague–Dawley rats: implications of decreased glucuronidation in obese Zucker rats. Drug Metab. Dispos. 32, 909–914.

Kimoto, E., Seki, S., Itagaki, S., Matsuura, M., Kobayashi, M., Hirano, T., Goto, Y., Tadano, K., Iseki, K., 2007. Efflux transport of *N*-monodesethylamiodarone by the human intestinal cell-line Caco-2 cells. Drug Metab. Pharmacokinet. 22, 307–312.

Korashy, H.M., El-Kadi, A.O., 2004. Differential effects of mercury, lead and copper on the constitutive and inducible expression of aryl hydrocarbon receptor (AHR)-regulated genes in cultured hepatoma Hepa 1c1c7 cells. Toxicology 201, 153–172.

Lowry, O.H., Rosebrough, N.J., Farr, A.L., Randall, R.J., 1951. Protein measurement with the Folin phenol reagent. J. Biol. Chem. 193, 265–275.

Omura, T., Sato, R., 1964. The carbon monoxide-binding pigment of liver microsomes. Ii. Solubilization, purification, and properties. J. Biol. Chem. 239, 2379–2385.

Palmer, W.K., Emeson, E.E., Johnston, T.P., 1997. The poloxamer 407-induced hyperlipidemic atherogenic animal model. Med. Sci. Sports Exerc. 29, 1416–1421.

Pascussi, J.M., Gerbal-Chaloin, S., Drocourt, L., Maurel, P., Vilarem, M.J., 2003. The expression of CYP2B6, CYP2C9 and CYP3A4 genes: a tangle of networks of nuclear and steroid receptors. Biochim. Biophys. Acta 1619, 243–253.

Plomp, T.A., Wiersinga, W.M., Maes, R.A., 1985. Tissue distribution of amiodarone and desethylamiodarone in rats after repeated oral administration of various amiodarone dosages. Arzneimittelforschung 35, 1805–1810.

Riva, E., Gerna, M., Latini, R., Giani, P., Volpi, A., Maggioni, A., 1982a. Pharmacokinetics of amiodarone in man. J. Cardiovasc. Pharmacol. 4, 264–269.

Riva, E., Gerna, M., Neyroz, P., Urso, R., Bartosek, I., Guaitani, A., 1982b. Pharmacokinetics of amiodarone in rats. J. Cardiovasc. Pharmacol. 4, 270–275.

Sermsappasuk, P., Baek, M., Weiss, M., 2006. Kinetic analysis of myocardial uptake and negative inotropic effect of amiodarone in rat heart. Eur. J. Pharm. Sci. 28, 243–248.

Shayeganpour, A., Jun, A.S., Brocks, D.R., 2005. Pharmacokinetics of amiodarone in hyperlipidemic and simulated high fat-meal rat models. Biopharm. Drug Dispos. 26, 249–257.

Shayeganpour, A., El-Kadi, A.O., Brocks, D.R., 2006. Determination of the enzyme(s) involved in the metabolism of amiodarone in liver and intestine of rat: the contribution of cytochrome P450 3A isoforms. Drug Metab. Dispos. 34, 43–50.

Shayeganpour, A., Hamdy, D.A., Brocks, D.R., 2007a. Pharmacokinetics of desethylamiodarone in the rat after its administration as the preformed metabolite, and after administration of amiodarone. Biopharm. Drug Dispos. 29, 159–166.

Shayeganpour, A., Lee, S.D., Wasan, K.M., Brocks, D.R., 2007b. The influence of hyperlipoproteinemia on in vitro distribution of amiodarone and desethylamiodarone in human and rat plasma. Pharm. Res. 24, 672–678.

Shayeganpour, A., Somayaji, V., Brocks, D.R., 2007c. A liquid chromatography-mass spectrometry assay method for simultaneous determination of amiodarone and desethylamiodarone in rat specimens. Biomed. Chromatogr. 21, 284–290.

Talajic, M., Nattel, S., Davies, M., McCans, J., 1989. Attenuation of class 3 and sinus node effects of amiodarone by experimental hypothyroidism. J. Cardiovasc. Pharmacol. 13, 447–450.

Tiebel, O., Oka, K., Robinson, K., Sullivan, M., Martinez, J., Nakamuta, M., Ishimura-Oka, K., Chan, L., 1999. Mouse very low-density lipoprotein receptor (VLDLR): gene structure, tissue-specific expression and dietary and developmental regulation. Atherosclerosis 145, 239–251.

Vadiei, K., Lopez-Berestein, G., Luke, D.R., 1990. Disposition and toxicity of amphotericin-B in the hyperlipidemic Zucker rat model. Int. J. Obes. 14, 465–472.

Varbiro, G., Toth, A., Tapodi, A., Bognar, Z., Veres, B., Sumegi, B., Gallyas Jr., F., 2003. Protective effect of amiodarone but not *N*-desethylamiodarone on postischemic hearts through the inhibition of mitochondrial permeability transition. J. Pharmacol. Exp. Ther. 307, 615–625.

Vassallo, P., Trohman, R.G., 2007. Prescribing amiodarone: an evidence-based review of clinical indications. JAMA 298, 1312–1322.

Vuppugalla, R., Mehvar, R., 2005. Enzyme-selective effects of nitric oxide on affinity and maximum velocity of various rat cytochromes P450. Drug Metab. Dispos. 33, 829–836.

Wasan, K.M., Subramanian, R., Kwong, M., Goldberg, I.J., Wright, T., Johnston, T.P., 2003. Poloxamer 407-mediated alterations in the activities of enzymes regulating lipid metabolism in rats. J. Pharm. Pharm. Sci. 6, 189–197.

Wasan, K.M., Brocks, D.R., Lee, S.D., Sachs-Barrable, K., Thornton, S.J., 2008. Impact of lipoproteins on the biological activity and disposition of hydrophobic drugs: implications for drug discovery. Nat. Rev. Drug Discov. 7, 84–99.

Weiss, M., 1999. The anomalous pharmacokinetics of amiodarone explained by nonexponential tissue trapping. J. Pharmacokinet. Biopharm. 27, 383–396.

Wyss, P.A., Moor, M.J., Bickel, M.H., 1990. Single-dose kinetics of tissue distribution, excretion and metabolism of amiodarone in rats. J. Pharmacol. Exp. Ther. 254, 502–507.

Xiong, H., Yoshinari, K., Brouwer, K.L., Negishi, M., 2002. Role of constitutive androstane receptor in the in vivo induction of Mrp3 and CYP2B1/2 by phenobarbital. Drug Metab. Dispos. 30, 918–923.

Yoshinari, K., Takagi, S., Yoshimasa, T., Sugatani, J., Miwa, M., 2006. Hepatic CYP3A expression is attenuated in obese mice fed a high-fat diet. Pharm. Res. 23, 1188–1200.